Phytochemistry Letters 41 (2021) 38–42

Contents lists available at ScienceDirect

Phytochemistry Letters

journal homepage: www.elsevier.com/locate/phytol

Tetrahydroprotoberberine *N*-oxides from *Chelidonium majus* and their inhibitory effects on NO production in RAW 264.7 cells

Thi Phuong Linh Le [a], Jin Woo Lee [a], Jun Gu Kim [a], Jae Sang Han [a], Haeun Kwon [b], Dongho Lee [b], Mi Kyeong Lee [a], Bang Yeon Hwang [a,*]

[a] College of Pharmacy, Chungbuk National University, Cheongju, 28160, Republic of Korea
[b] Department of Plant Biotechnology, College of Life Sciences and Biotechnology, Korea University, Seoul, 02841, Republic of Korea

ARTICLE INFO

Keywords:
Chelidonium majus
Papaveraceae
Nitric oxide, tetrahydrocoptisine *N*-oxide

ABSTRACT

Two new tetrahydroprotoberberine *N*-oxides, 7*R*,14*S*-*cis*-tetrahydrocoptisine *N*-oxide (**1**) and 7*R*,14*R*-*trans*-tetrahydrocoptisine *N*-oxide (**2**) along with fourteen known compounds (**3**–**16**) were isolated from the aerial parts of *Chelidonium majus*. Their structures were elucidated by spectroscopic and spectrometric methods, such as 1D and 2D-NMR (HSQC, HMBC, NOESY) and HRESIMS. The absolute configurations of **1** and **2** were established by comparison of their experimental and calculated ECD data. All isolates were evaluated for their inhibitory effects on the nitric oxide production in LPS-induced RAW 264.7 macrophages, and compounds **2**, **6**–**10**, **13**, and **15** showed significant inhibitory effects with the IC_{50} values ranging from 1.1–31.9 μM.

1. Introduction

Chelidonium majus L., a perennial and herbaceous plant belongs to the family Papaveraceae, is distributed widely in the temperate region of Asia, Europe, and North Africa. It has been used traditionally in Korean folk medicine to treat liver diseases, gastric cancer, gastric ulcer, oral infection, tuberculosis, jaundice, and various skin disorders (Barnes et al., 2007; Gilca et al., 2010). Previous phytochemical studies of *C. majus* have revealed the presence of many types of alkaloids such as benzo[*c*]phenanthridine, protopine, and protoberberine (Colombo and Bosisio, 1996; Gu et al., 2010). Some of these compounds have been found to exhibit anti-inflammatory, anti-microbial, immunomodulatory, anti-cancer, and anti-oxidant activities (Lenfeld et al., 1981; Meng et al., 2009; Kim et al., 2013; Zhang et al., 2014; Capistrano et al., 2015; Havelek et al., 2016). As a part of a program to search for the plant-derived anti-inflammatory compounds, a MeOH extract of the aerial parts of *C. majus* was examined for inhibitory effects on lipopolysaccharide (LPS)-induced nitric oxide (NO) production in RAW 264.7 macrophages (IC_{50} value: 31.5 μg/mL). Chromatographic isolation yielded two new tetrahydroprotoberberine *N*-oxides, 7*R*,14*S*-*cis*--tetrahydrocoptisine *N*-oxide (**1**) and 7*R*,14*R*-*trans*-tetrahydrocoptisine *N*-oxide (**2**) and fourteen known compounds (**3**-**16**) (Fig. 1). Herein are described the isolation and structure determination of the new compounds and the inhibitory effects of compounds **1**-**16** on NO production in LPS-induced RAW 264.7 cells.

2. Results and discussion

Compound **1** was obtained as a white amorphous powder. Its molecular formula was determined as $C_{19}H_{17}NO_5$ from the HRESIMS (*m/z* 340.1179 $[M+H]^+$, calcd 340.1185) and ^{13}C NMR data, indicating the presence of 12 degrees of unsaturation. The ^1H NMR data (Table 1) suggested the presence of two singlet aromatic protons at δ_H 6.73 (1H, s, H-1) and 6.72 (1H, s, H-4), two *ortho*-coupled aromatic protons at δ_H 6.79 (1H, d, J = 8.1 Hz, H-11) and 6.73 (1H, d, J = 8.1 Hz, H-12), two methylenedioxy groups at δ_H 5.92 (1H, d, J = 1.1 Hz, H-15a), 5.91 (1H, d, J = 1.1 Hz, H-15b), 5.96 (1H, d, J = 1.1 Hz, H-16a), and 6.01 (1H, d, J = 1.1 Hz, H-16b). Four mutually coupling protons at δ_H 3.04 (H-5β), 3.41 (H-6α), 3.44 (H-5α), and 3.83 (H-6β) in ring B, and three other mutually coupling protons at δ_H 3.13 (1H, dd, J = 18.0, 9.2 Hz, H-13β), 3.65 (1H, dd, J = 18.0, 5.8 Hz, H-13α), and 4.58 (1H, m, H-14) in ring C were also observed. The ^{13}C NMR data in combination with HSQC spectrum revealed the presence of 19 carbon signals, corresponding to twelve aromatic carbons, two methylenedioxy carbons (δ_C 102.6 and 103.2), two *N*-methylene carbons (δ_C 59.1 and 64.7), two methylene carbons (δ_C 26.2 and 36.2), and a *N*-methine carbon (δ_C 72.5) (Table 1). The aforementioned evidence and information from the HRESIMS data suggested that **1** possesses a 2,3,9,10-oxygenated

* Corresponding author.
E-mail address: byhwang@chungbuk.ac.kr (B.Y. Hwang).

https://doi.org/10.1016/j.phytol.2020.10.014
Received 29 July 2020; Received in revised form 18 September 2020; Accepted 23 October 2020
Available online 5 November 2020
1874-3900/© 2020 Phytochemical Society of Europe. Published by Elsevier Ltd. All rights reserved.

tetrahydroprotoberberine skeleton with *N*-oxide and two methylenedioxy groups (Chen et al., 1999, 2001). The locations of two methylenedioxy groups were assigned at C-2/C-3 and C-9/C-10, respectively, based on the HMBC correlations observed from CH_2-15 (δ_H 5.92 and 5.91) to C-2 (δ_C 149.0) and C-3 (δ_C 148.0), as well as from CH_2-16 (δ_H 5.96 and 6.01) to C-9 (δ_C 145.2) and C-10 (δ_C 147.7) (Fig. 2). The relative configuration at the B/C ring junction was established by comparison of ^{13}C NMR data of compound **1** with those of related compounds, *cis*- and *trans*-corydalmine *N*-oxide and *cis*- and *trans*-canadine *N*-oxide (Hussain et al., 1983; Chen et al., 1999, 2001). The chemical shifts at δ_C 59.1 (C-6), 36.2 (C-13), and 72.5 (C-14) observed for compound **1** were indicative of a *cis*-tetrahydrocoptisine-*N*-oxide configuration, whereas the chemical shifts for the *trans*-tetrahydrocoptisine-*N*-oxide as in compound **2** would be at δ_C 65.1 (C-6), 30.8 (C-13), and 69.6 (C-14). The relative configuration was established by the NOESY correlations between H-1/H-14/H_2-13, H-14/H-13α/H-8α, H-12/H_2-13, H-4/H_2-5, and H_2-6/H-8β (Fig. 2). The absolute configuration at N-7 and C-14 was established by electronic circular dichroism (ECD) calculation analyses using time-dependent density functional theory (TDDFT), and the measured ECD spectrum for 7*R*, 14*S* matched well with the calculated ECD spectrum (Fig. 3). Therefore, the structure of **1** was determined to be (5*R*,12b*S*)-4,5,6,7, 12b,13-hexahydro-[1,3]dioxolo[4′,5′:7,8]isoquinolino[3,2-*a*][1,3]dioxolo[4,5-*g*]isoquinoline 5-oxide and named 7*R*,14*S*-*cis*-tetrahydrocoptisine *N*-oxide.

Compound **2** was isolated as a white amorphous powder having a molecular formula of $C_{19}H_{17}NO_5$, the same as **1**, based on the HRESIMS (*m/z* 340.1179 $[M+H]^+$, calcd 340.1185) and ^{13}C NMR data (Table 1). The ^{1}H- and ^{13}C NMR data closely resembled those of **1**, with the only differences in the chemical shifts at C-6 (δ_C 65.1), C-13 (δ_C 30.8), and C-14 (δ_C 69.6), suggesting a *trans* configuration at the B/C ring junction. Comprehensive analysis of 2D-NMR (COSY, HSQC, and HMBC) data confirmed that the planar structure was the same as those of (-)-tetrahydrocoptisine *N*-oxide, which was recently isolated from the aerial part of *C. majus* without determination of the absolute configuration (Huang et al., 2019). Compound **2** showed NOESY correlations between H-1/H_2-13, H-14/H-5β/H-6β/H-8β/H-13β, H-12/H_2-13, H-4/H-5α, and H-6β/H-8β, which proved the relative configuration (Fig. 2). The absolute configuration was further confirmed by ECD calculation, in which the experimental ECD spectrum matched well with that calculated for 7*R*,14*R*. Therefore, the structure of **2** was determined to be (5*R*,12b*R*)-4, 5,6,7,12b,13-hexahydro-[1,3]dioxolo[4′,5′:7,8]isoquinolino[3,2-*a*][1, 3]dioxolo[4,5-*g*]isoquinoline 5-oxide and named 7*R*,14*R*-*trans*-tetrahydrocoptisine *N*-oxide.

The structures of the known compounds were identified as impatien B (**3**) (Li et al., 2013), spallidamine (**4**) (Ito et al., 1990; Sai et al., 2016), oxychelerythrine (**5**) (Le and Cho, 2006; Miao et al., 2011), dihydrosanguinarine (**6**) (Miao et al., 2011), *N*-demethyloxysanguinarine (**7**) (Chang et al., 2003), chelidonine (**8**) (Ito et al., 2011), isochelidonine (**9**) (De Rosa and Di Vincenzo, 1992), *trans*-coumaroyltyramine (**10**) (Song et al., 2016), *cis*-coumaroyltyramine (**11**) (Kim et al., 2005), *trans*-*N*-feruloyltyramine (**12**) (Song et al., 2016), 4-[formyl-5-methoxymethyl-1*H*-pyrol-1-yl] butanoate (**13**) (Chin et al., 2003), noroxyhydrastinine (**14**) (Cho et al., 2006), 3,4-dehydrotheaspirone (**15**) (Moujir et al., 2011), and loliolide (**16**) (Kimura and Maki, 2002) by comparison of their spectroscopic (UV, 1D and 2D NMR) and ESIMS data with those of published values.

Table 1
^{1}H and ^{13}C NMR data of compounds **1** and **2**.[a]

Position	**1**			**2**	
	δ_H (*J* in Hz)[b]	δ_C[b]	δ_C[c]	δ_H (*J* in Hz)[b]	δ_C[b]
1	6.73, s	107.8	107.5	6.88, s	106.8
1a	–	128.1	128.6	–	127.3
2	–	149.0	147.1	–	148.7
3	–	148.0	146.3	–	147.3
4	6.72, s	109.6	109.2	6.71, s	109.2
4a	–	125.0	125.3	–	126.8
5α	3.44, m	26.2	26.1	2.83, dd, (16.8, 3.7)	25.5
5β	3.04, dd, (15.1, 7.6)			3.63, dd, (13.5, 5.7)	
6α	3.41, m	59.1	59.1	3.76, m	65.1
6β	3.83, m			3.84, m	
8α	4.59, m	64.7	63.6	4.48, d, (15.0)	66.4
8β	4.64, d, (16.0)			4.76, d, (15.0)	
8a	–	112.4	113.0	–	112.3
9	–	145.2	143.9	–	145.7
10	–	147.7	146.1	–	148.6
11	6.79, d, (8.1)	109.4	108.5	6.84, d, (8.0)	108.8
12	6.73, d, (8.1)	122.1	121.5	6.80, d, (8.0)	122.3
12a	–	124.7	124.9	–	126.2
13α	3.65, dd, (18.0, 5.8)	36.2	34.5	3.60, dd, (16.6, 4.3)	30.8
13β	3.13, dd, (18.0, 9.2)			3.29, m	
14	4.58, m	72.5	71.2	4.88, m	69.6
15	5.92, d, (1.1)	102.6	102.2	5.94, br s	102.7
	5.91, d, (1.1)			5.95, br s	
16	5.96, d, (1.1)	103.2	101.6	5.96, br s	103.0
	6.01, d, (1.1)			6.01, br s	

[a] Assignments were supported with HSQC, HMBC and NOESY experiments.
[b] Measured in CD_3OD at 700 MHz for ^{1}H NMR and at 175 MHz for ^{13}C NMR.
[c] Measured in DMSO-d_6 at 100 MHz for ^{13}C NMR.

All isolates (**1–16**) were tested for their inhibitory effects on the NO production in LPS-induced RAW 264.7 cells, with aminoguanidine as the positive control. None of the tested compounds showed any cytotoxicity at their effective concentration for the inhibition of NO production (data not shown). Of these, dihydrosanguinarine (**6**), a benzophenanthridine alkaloid mainly found in the family Papaveraceae, was found to exhibit significant inhibitory effect with an IC_{50} value of 1.1 μM. Three benzophenanthridine alkaloids, such as *N*-demethyloxysanguinarine (**7**), chelidonine (**8**), and isochelidonine (**9**) also showed inhibitory effects with IC_{50} value of 11.6, 21.4, and 31.9 μM, respectively. Compound **2** showed stronger inhibitory effect (IC_{50} 26.3 μM) on LPS-induced NO production than that of compound **1** (IC_{50} >100 μM) (Table 2). Interestingly, compounds **1** and **2** differ only in the configuration of the B/C

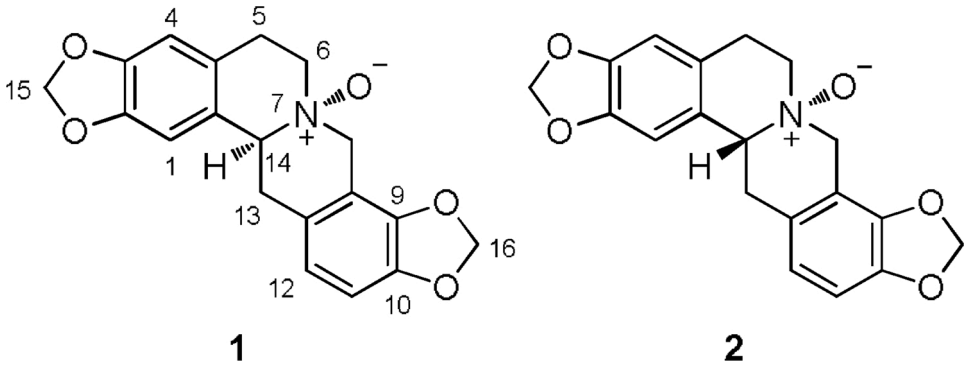

Fig. 1. Chemical structures of compounds **1** and **2.**

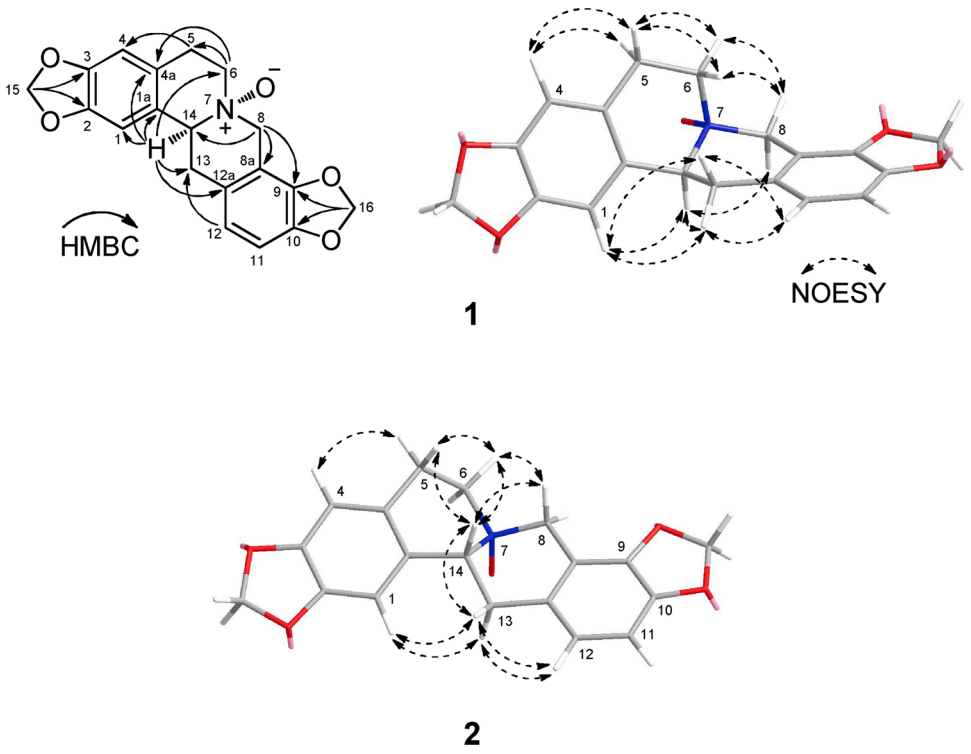

Fig. 2. Key HMBC and NOESY correlations of compounds **1** and **2.**

ring junction, implying that the 3D conformation of these compounds could probably play an important role for the NO inhibition. *Trans*-coumaroyltyramine (**10**), 4-[formyl-5-methoxymethyl-1*H*-pyrol-1-yl] butanoate (**13**), and 3,4-dehydrotheaspirone (**15**) also showed moderate inhibitory effects with IC_{50} value of 25.3, 21.1, and 23.4 μM, respectively. Several isoquinoline alkaloids such as chelidonine, norchelidonine, and 8-hydroxydihydrosanguinarine from *C. majus* were found to have inhibitory effects on NO production (Park et al., 2011). Chelidonic acid inhibited the production of IL-6 and the expression of IL-6 mRNA by blocking NF-κB (Shin et al., 2011). In addition, chelidonine suppressed the production of LPS-induced NO and PGE_2, as well as iNOS and COX-2 mRNA and protein expression, by inhibiting the TLR4/NF-κB signaling pathway (Liao et al., 2018). Stylopine from *C. majus* also suppressed the production of NO, PGE_2, TNF-α, IL-1β, and IL-6, and the expression of iNOS and COX-2 in LPS-stimulated RAW 264.7 cells (Jang et al., 2004).

In conclusion, the present study supports the medicinal use of *C. majus* in the cure of inflammatory diseases, as well as the contribution of isoquinoline alkaloids to the anti-inflammatory activity of this plant. The aerial parts of *C. majus* may be useful for the treatment of inflammatory diseases caused by excessive production of NO.

3. Experimental

3.1. General experimental procedures

Gravity column chromatography was performed using a silica gel (Kieselgel 60, 70–230 mesh, Merck). TLC was performed using precoated silica gel 60 F_{254} (0.25 mm, Merck), and spots were detected by a 10 % vanillin-H_2SO_4 in water spray reagent. MPLC was performed using a Biotage Isolera system with Lichroprep RP-18 (40−63 μm, Merck). Semi-preparative HPLC was performed using a Waters HPLC system (two Waters 515 pumps with a 2996 photodiode-array detector) with a YMC J'sphere ODS-H80 (4 μm, 150 × 20 mm, i.d.). Optical rotations were measured with a JASCO DIP-1000 polarimeter. UV spectra were recorded on a JASCO UV-550 spectrophotometer. HRESIMS spectra were recorded on a maXis 4 G (Bruker, Germany) mass spectrometer. IR spectra were acquired on a JASCO FT-IR 4100 spectrometer. 1D and 2D NMR spectra were obtained on Bruker AVANCE III 500 and 700 MHz NMR spectrometers using $CDCl_3$, DMSO-d_6, and CD_3OD as solvents. ESIMS and HRESIMS were obtained on LCQ Fleet and maXis 4 G mass spectrometers, respectively. ECD spectra were obtained on a JASCO J-715 spectrometer.

3.2. Plant material

The dried aerial parts of *C. majus* were obtained from Kyungdong herbal market in Seoul, Korea, in March 2018. A voucher specimen (CBNU-2018-03-CM) was authenticated by B. Y. Hwang and deposited at the Herbarium of the College of Pharmacy, Chungbuk National University, Korea.

3.3. Extraction and isolation

The dried aerial parts of *C. majus* (3.0 kg) were powdered and extracted with MeOH (3 × 10 L) at room temperature for 3 days. After solvent was removed under reduced pressure, the residue was suspended in water and then partitioned with *n*-hexane, CH_2Cl_2, and EtOAc respectively. The CH_2Cl_2-soluble fraction (21.5 g) was chromatographed on a silica gel column (7 × 25 cm) using a stepwise gradient of CH_2Cl_2-EtOAc (1:0 to 0:1) to give eleven sub-fractions (CMC1 - CMC11). Fraction CMC5 was chromatographed further on a silica gel column (5 × 40 cm) using a gradient solvent system of CH_2Cl_2-MeOH (50:1 to 0:1) to give eight sub-fractions (CMC5A - CMC5H). Fraction CMC5B was purified by MPLC on a Lichroprep RP-18 column (CH_3CN-H_2O, 10:90 to 80:20) to afford eleven sub-fractions (CMC5B1 - CMC5B11). Fraction CMC5B5 was further purified by semi-preparative HPLC (CH_3CN-H_2O, 20:80 to 60:40, 6 mL/min) to yield compounds **1** (t_R = 14.5 min, 3.0 mg), **2** (t_R = 17.6 min, 9.3 mg), **3** (t_R = 20.3 min, 1.9 mg), and **4** (t_R = 42.3 min, 2.7 mg). Fraction CMC6 was chromatographed on a silica gel column (4 × 45 cm) using a gradient solvent system of CH_2Cl_2-MeOH (30:1 to 0:1) to give six sub-fractions (CMC6A - CMC6F). Fraction CMC6A was separated by MPLC on a Lichroprep RP-18 column (MeOH-

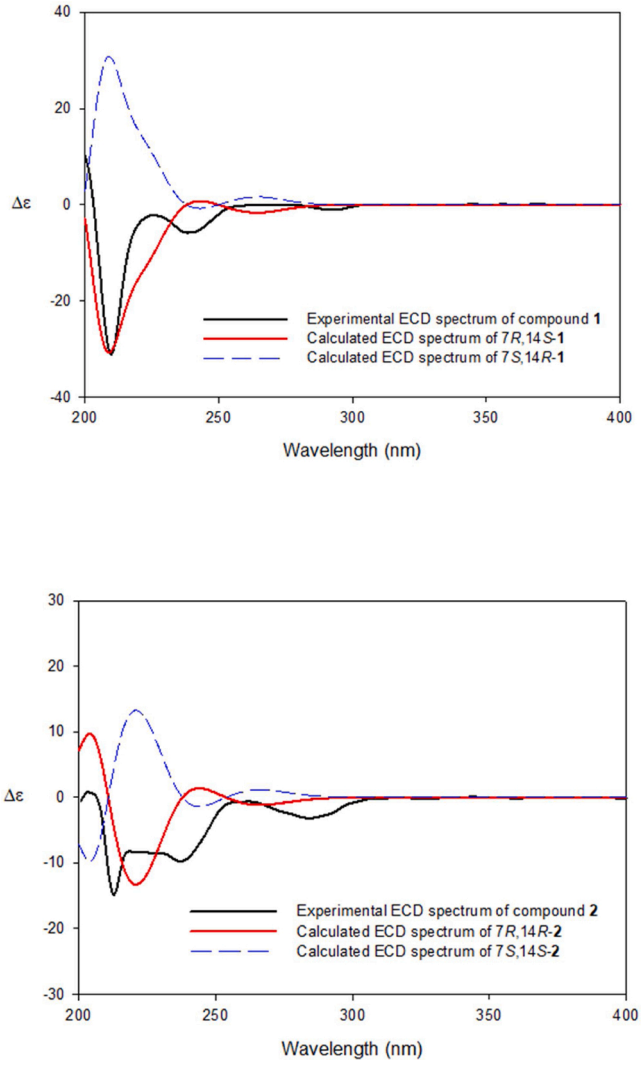

Fig. 3. Experimental and calculated ECD spectra of compounds **1** and **2.**

Table 2
Inhibitory effects of compounds **1-16** on LPS-induced NO production in RAW 264.7 cells.

Compound	IC_{50} (μM)[a]	Compound	IC_{50} (μM)
1	> 100	9	31.9 ± 6.98
2	26.3 ± 2.03	10	25.3 ± 0.34
3	> 100	11	> 100
4	> 100	12	47.0 ± 0.66
5	70.1 ± 5.18	13	21.1 ± 3.18
6	1.1 ± 0.56	14	> 100
7	11.6 ± 3.18	15	23.4 ± 2.29
8	21.4 ± 2.29	16	47.5 ± 7.81

* Aminoguanidine was used as the positive control (IC_{50}: 15.9 μM).
[a] Results are expressed as the mean ± SD in μM from three independent experiments.

H_2O, 10:90 to 90:10) to afford seven sub-fractions (CMC6A1 - CMC6A7). Fraction CMC6A3 was purified by semi-preparative HPLC (CH_3CN-H_2O, 20:80 to 60:40, 6 mL/min) to yield compounds **14** (t_R = 14.3 min, 5.0 mg) and **16** (t_R = 16.3 min, 8.5 mg). Fraction CMC3 was further purified by semi-preparative HPLC (CH_3CN-H_2O, 25:75 to 90:10, 6 mL/min) to yield compound **5** (t_R = 25.3 min, 2.0 mg). Fraction CMC9 was chromatographed on a silica gel column (4 × 45 cm) eluted with a step gradient of CH_2Cl_2 - EtOAc (1:0 to 0:1) to give six sub-fractions (CMC9A - CMC9F). Fraction CMC9A was purified by semi-preparative HPLC (CH_3CN-H_2O, 45:55 to 65:35, 6 mL/min) to afford compound **6** (t_R = 28.7 min, 2.1 mg). Fraction CMC9C was separated by MPLC with a Lichroprep RP-18 column and a CH_3CN - H_2O gradient system (20:80 to 100:0) to give five sub-fractions (CMC9C1 - CMC9C5). Fraction CMC9C3 was purified by semi-preparative HPLC (CH_3CN-H_2O, 40:60 to 65:35, 6 mL/min) to afford compound **7** (t_R = 19.1 min, 3.0 mg). Fraction CMC10 was fractionated by MPLC on a Lichroprep RP-18 column eluted with CH_3CN-H_2O gradient (20:80 to 100:0) to give six sub-fractions (CMC10A–CMC10F). Fraction CMC10D was chromatographed on a silica gel (CH_2Cl_2-MeOH, 30:1 to 0:1) to afford compound **8** (212 mg). Fractions CMC10E was chromatographed on a silica gel column (CH_2Cl_2-EtOAc, 20:1 to 1:1) to afford compound **9** (8.0 mg). Fraction CMC11 was chromatographed on a silica gel column and eluted with CH_2Cl_2-MeOH gradient (50:1 to 1:1) to give six sub-fractions (CMC11A - CMC11F). Fraction CMC11C was purified by semi-preparative HPLC (CH_3CN-H_2O, 20:80 to 40:60, 6 mL/min) to afford compound **15** (t_R = 14.0 min, 1.0 mg). Fraction CMC11D was further purified by semi-preparative HPLC (CH_3CN-H_2O, 20:80 to 50:50, 6 mL/min) to give compound **12** (t_R = 17.9 min, 13.6 mg).

The EtOAc-soluble fraction (2.8 g) was chromatographed on a silica gel column (5 × 45 cm) and eluted with CH_2Cl_2-MeOH gradient (100:1 to 0:1) to give seven sub-fractions (CME1 - CME7). Fraction CME5 was fractionated on a silica gel column with CH_2Cl_2-MeOH gradient (100:1 to 5:1) to give four sub-fractions (CME5A - CME5D). Fraction CME5B was purified by semi-preparative HPLC (CH_3CN-H_2O, 15:85 to 50:50, 6 mL/min) to give compounds **10** (t_R = 19.1 min, 5.2 mg) and **11** (t_R = 20.3 min, 3.5 mg). Fraction CME2 was separated by MPLC on a Lichroprep RP-18 column (CH_3CN-H_2O, 10:90 to 100:0) to give five sub-fractions (CME2A - CME2E). Fraction CME2D was further purified by semi-preparative HPLC (CH_3CN-H_2O, 35:65 to 80:20, 6 mL/min) to afford compound **13** (t_R = 15.6 min, 2.1 mg).

3.3.1. *7R,14S-cis-tetrahydrocoptisine N-oxide (1)*

White amorphous powder; $[\alpha]^{25}_D$ -29.2 (*c* 0.10, MeOH); UV (MeOH) λ_{max} (log ε): 207 (4.65), 236 (3.75), 287 (3.68) nm; IR (KBr) ν_{max} (cm^{-1}): 1602, 1505, 1450; ECD (MeOH) λ_{max} (Δε) 213 (-33.6), 238 (-11.7) and 293 (-4.95) nm; ^1H (700 MHz, CD_3OD) and ^{13}C (175 MHz, CD_3OD) NMR data, see Table 1; HRESIMS *m/z* 340.1179 $[M+H]^+$

3.3.2. *7R,14R-trans-tetrahydrocoptisine N-oxide (2)*

White amorphous powder; $[\alpha]^{25}_D$ -28.1 (*c* 0.10, MeOH); UV (MeOH) λ_{max} (log ε): 210 (4.57), 238 (3.69), 288 (3.58) nm; IR (KBr) ν_{max} (cm^{-1}): 1605, 1502, 1458; ECD (MeOH) λ_{max} (Δε) 213 (-18.0), 226 (-8.49), 238 (-8.84) and 285 (-5.18) nm; ^1H (700 MHz, CD_3OD) and ^{13}C (175 MHz, CD_3OD) NMR data, see Table 1; HRESIMS *m/z* 340.1179 $[M+H]^+$

3.4. *Determination of LPS-induced NO production and cell viability*

The nitrite concentration in the culture medium was measured as an indicator of NO production according to the Griess reaction. Briefly, RAW 264.7 cells were seeded into 96-well tissue culture plates at 2×10^6 cells/mL, and stimulated with 1 μg/mL of LPS in the presence or absence of test compounds. After incubation at 37 °C for 24 h, 100 μL of cell-free supernatant were mixed with 100 μL of Griess reagent containing equal volumes of 2 % (w/v) sulfanilamide in 5 % (w/v) phosphoric acid and 0.2 % (w/v) of *N*-(1-naphthyl)ethylenediamine solution to determine nitrite production. Absorbance was measured at 550 nm against a calibration curve with sodium nitrite standards. Cell viability of the remaining cells was determined by MTT (Sigma Chemical Co., St. Louis, MO)-based colorimetric assay.

3.5. *Computational method*

The conformer distribution was conducted by an MMFF force field with Spartan'14 software (Wave-function, Inc., Irvine, CA, USA). The geometry optimization for selected conformers were performed at DFT

[B3LYP functional/6-31+G(d,p) basis set] level, and ECD calculations were accomplished at TDDFT (CAM-B3LYP/SVP basis set) level with a CPCM solvent model in Acetonitrile by Gaussian 09 software (Gaussian, Inc., Wallingford, CT, USA). The calculated ECD curves were simulated by SpecDis 1.64 software (University of Wuerzburg, Wuerzburg, Germany) with a half bandwidth of 0.3 eV. ECD curves of conformers were weighted using the Boltzmann distribution after UV correction (Kwon et al., 2016).

Declaration of Competing Interest

The authors declare that there are no conflicts of interest.

Acknowledgments

This work was supported by the National Research Foundation of Korea (NRF) grant funded by the Korea government (MIST) (No. 2020R1A2C1008406), the Medical Research Center Program (MRC, 2017R1A5A2015541) through the National Research Foundation of Korea, and by the Korea Basic Science Institute under the R&D program (Project No. C030440) supervised by the Ministry of Science and ICT.

Appendix A. Supplementary data

Supplementary material related to this article can be found, in the online version, at doi:https://doi.org/10.1016/j.phytol.2020.10.014.

References

Barnes, J., Anderson, L., Philipson, D., 2007. Herbal Medicines: A Guide for Healthcare. Pharmaceutical Press, London, pp. 136–145.
Capistrano, I.R., Wouters, A., Lardon, F., Gravekamp, C., Apers, S., Pieters, L., 2015. *In vitro* and *in vivo* investigations on the antitumour activity of *Chelidonium majus*. Phytomedicine 22, 1279–1287.
Chang, Y.C., Chang, F.R., Khalil, A.T., Hsieh, P.W., Wu, Y.C., 2003. Cytotoxic benzophenanthridine and benzylisoquinoline alkaloids from *Argemone mexicana*. Z. Naturforsch. C 58, 521–526.
Chen, J.J., Duh, C.Y., Chen, I.S., 1999. New tetrahydroprotoberberine *N*-oxide alkaloids and cytotoxic constituents of *Corydalis tashiroi*. Planta Med. 65, 643–647.
Chen, J.J., Chang, Y.L., Teng, C.M., Lin, W.Y., Chen, Y.C., Chen, I.S., 2001. A new tetrahydroprotoberberine *N*-oxide alkaloid and anti-platelet aggregation constituents of *Corydalis tashiroi*. Planta Med. 67, 423–427.
Chin, Y.W., Lim, S.W., Kim, S.H., Shin, D.Y., Suh, Y.G., Kim, Y.B., Kim, Y.C., Kim, J., 2003. Hepatoprotective pyrrole derivatives of *Lycium chinense* fruits. Bioorg. Med. Chem. Lett. 13, 79–81.
Cho, K.M., Yoo, I.D., Kim, W.G., 2006. 8-hydroxydihydrochelerythrine and 8-hydroxy-dihydrosanguinarine with a potent acetylcholinesterase inhibitory activity from *Chelidonium majus* L. Biol. Pharm. Bull. 29, 2317–2320.
Colombo, M.L., Bosisio, E., 1996. Pharmacological activities of *Chelidonium majus* L. (Papaveraceae). Pharmacol. Res. 33, 127–134.
De Rosa, S., Di Vincenzo, G., 1992. Isochelidonine, a benzophenanthridine alkaloid from *Chelidonium majus*. Phytochemistry 31, 1085–1086.
Gilca, M., Gaman, L., Panait, E., Stoian, I., Atanasiu, V., 2010. *Chelidonium majus* - an integrative review: traditional knowledge versus modern findings. Forsch. 17, 241–248.
Gu, Y., Qian, D., Duan, J.A., Wang, Z., Guo, J., Tang, Y., Guo, S., 2010. Simultaneous determination of seven main alkaloids of *Chelidonium majus* L. by ultra-performance LC with photodiode-array detection. J. Sep. Sci. 33, 1004–1009.
Havelek, R., Seifrtova, M., Kralovec, K., Krocova, E., Tejkalova, V., Novotny, I., Cahlikova, L., Safratova, M., Opletal, L., Bilkova, Z., Vavrova, J., Rezacova, M., 2016. Comparative cytotoxicity of chelidonine and homochelidonine, the dimethoxy analogues isolated from *Chelidonium majus* L. (Papaveraceae), against human leukemic and lung carcinoma cells. Phytomedicine 23, 253–266.
Huang, X.Y., Shao, Z.X., An, L.J., Xue, J.J., Li, D.H., Li, Z.L., Hua, H.M., 2019. New lignanamides and alkaloids from *Chelidonium majus* and their anti-inflammation activity. Fitoterapia 139, 104359.
Hussain, S.F., Gözler, B., Fajardo, V., Freyer, A.J., Shamma, M., 1983. The stereochemistry and ^{13}C NMR spectra of protopinium salts. J. Nat. Prod. 46, 251–255.
Ito, C., Mizuno, T., Wu, T.S., Furukawa, H., 1990. Alkaloids from *Corydalis*. Phytochemistry 29, 2044–2045.
Ito, M., Konno, F., Kumamoto, T., Suzuki, N., Kawahata, M., Yamaguchi, K., Ishikawa, T., 2011. Enantioselective synthesis of chelidonine, a B/C-cis-11-hydroxyhexahydrobenzo-[c]phenanthridine alkaloid. Tetrahedron 67, 8041–8049.
Jang, S.I., Kim, B.H., Lee, W.Y., An, S.J., Choi, H.G., Jeon, B.H., Chung, H.T., Rho, J.R., Kim, Y.J., Chai, K.Y., 2004. Stylopine from *Chelidonium majus* inhibits LPS-induced inflammatory mediators in RAW 264.7 cells. Arch. Pharm. Res. 27, 923–929.
Kim, D.K., Lim, J.P., Kim, J.W., Park, H.W., Eun, J.S., 2005. Antitumor and antiinflammatory constituents from *Celtis sinensis*. Arch. Pharm. Res. 28, 39–43.
Kim, D.H., Lee, J.H., Park, S., Oh, S.S., Kim, S., Kim, D.W., Park, K.H., Kim, K.D., 2013. 6-Acetonyl-5,6-dihydrosanguinarine (ADS) from *Chelidonium majus*L. triggers proinflammatory cytokine production via ROS-JNK/ERK-NFκB signaling pathway. Food Chem. Toxicol. 58, 273–279.
Kimura, J., Maki, N., 2002. New loliolide derivatives from the brown alga *Undaria pinnatifida*. J. Nat. Prod. 65, 57–58.
Kwon, J., Hiep, N.T., Kim, D.W., Hong, S., Guo, Y., Hwang, B.Y., Lee, H.J., Mar, W., Lee, D., 2016. Chemical constituents isolated from the root bark of *Cudrania tricuspidata* and their potential neuroprotective effects. J. Nat. Prod. 79, 1938–1951.
Le, T.N., Cho, W.J., 2006. A concise synthesis of 8-oxoberberine and oxychelerythrine, natural isoquinoline alkaloids through biomimetic synthetic way. Bull. Korean Chem. Soc. 27, 2093–2096.
Lenfeld, J., Kroutil, M., Marsálek, E., Slavík, J., Preininger, V., Simánek, V., 1981. Antiinflammatory activity of quaternary benzophenanthridine alkaloids from *Chelidonium majus*. Planta Med. 43, 161–165.
Li, J.C., Lin, Y.H., Hou, Y., Li, P., Xu, C.T., Li, G.P., 2013. Another new alkaloid from *Corydalis impatiens*. Asian J. Chem. 25, 585–586.
Liao, W., He, X., Yi, Z., Xiang, W., Ding, Y., 2018. Chelidonine suppresses LPS-induced production of inflammatory mediators through the inhibition of the TLR4/NF-κB signaling pathway in RAW264.7 macrophages. Biomed. Pharmacother. 107, 1151–1159.
Meng, F., Zuo, G., Hao, X., Wang, G., Xiao, H., Zhang, J., Xu, G., 2009. Antifungal activity of the benzo[c]phenanthridine alkaloids from *Chelidonium majus* Linn against resistant clinical yeast isolates. J. Ethnopharmacol. 125, 494–496.
Miao, F., Yang, X.J., Zhou, L., Hu, H.J., Zheng, F., Ding, X.D., Sun, D.M., Zhou, C.D., Sun, W., 2011. Structural modification of sanguinarine and chelerythrine and their antibacterial activity. Nat. Prod. Res. 25, 863–875.
Moujir, L.M., Seca, A.M., Araujo, L., Silva, A.M., Barreto, M.C., 2011. A new natural spiro heterocyclic compound and the cytotoxic activity of the secondary metabolites from *Juniperus brevifolia* leaves. Fitoterapia 82, 225–229.
Park, J.E., Cuong, T.D., Hung, T.M., Lee, I., Na, M., Kim, J.C., Ryoo, S., Lee, J.H., Choi, J. S., Woo, M.H., Min, B.S., 2011. Alkaloids from *Chelidonium majus* and their inhibitory effects on LPS-induced NO production in RAW264.7 cells. Bioorg. Med. Chem. Lett. 21, 6960–6963.
Sai, C.M., Li, D.H., Li, S.G., Han, T., Guo, Y.Z., Pei, Y.H., Bai, J., Jing, Y.K., Li, Z.L., Hua, H.M., 2016. Racemic alkaloids from *Macleaya cordata*: structural elucidation, chiral resolution, and cytotoxic, antibacterial activities. RSC Adv. 6, 41173–41180.
Shin, H.J., Kim, H.L., Kim, S.J., Chung, W.S., Kim, S.S., Um, J.Y., 2011. Inhibitory effects of chelidonic acid on IL-6 production by blocking NF-kB and caspase-1 in HMC-1 cells. Immunopharmacol. Immunotoxicol. 33, 614–619.
Song, Y.H., Kim, D.W., Curtis-Long, M.J., Park, C., Son, M., Kim, J.Y., Yuk, H.J., Lee, K. W., Park, K.H., 2016. Cinnamic acid amides from *Tribulus terrestris* displaying uncompetitive α-glucosidase inhibition. Eur. J. Med. Chem. 114, 201–208.
Zhang, W.J., You, C.X., Wang, C.F., Fan, L., Wang, Y., Su, Y., Deng, Z.W., Du, S.S., 2014. One new alkaloid from *Chelidonium majus* L. Nat. Prod. Res. 28, 1873–1878.